The Astrophysical Journal Letters, 1001:L21 (8pp), 2026 April 10 https://doi.org/10.3847/2041-8213/ae5a36
© 2026. The Author(s). Published by the American Astronomical Society.
OPEN ACCESS

Metastability in Emergent Dark Energy: A New Framework Confronting Cosmological Observations

Xiaolei Li[1], Tonghua Liu[2], Tian-Nuo Li[3], Guo-Hong Du[3], Arman Shafieloo[4,5], and Marek Biesiada[6]
[1] College of Physics, Hebei Normal University, Shijiazhuang 050024, People's Republic of China
[2] School of Physics and Optoelectronic Engineering, Yangtze University, Jingzhou 434023, People's Republic of China
[3] Liaoning Key Laboratory of Cosmology and Astrophysics, College of Sciences, Northeastern University, Shenyang 110819, People's Republic of China; liutongh@yangtzeu.edu.cn
[4] Korea Astronomy and Space Science Institute, Daejeon 34055, Republic of Korea; shafieloo@kasi.re.kr
[5] University of Science and Technology, Yuseong-gu 217 Gajeong-ro, Daejeon 34113, Republic of Korea
[6] National Centre for Nuclear Research, Pasteura 7, 02-093 Warsaw, Poland; Marek.Biesiada@ncbj.gov.pl
Received 2026 February 11; revised 2026 March 26; accepted 2026 April 1; published 2026 April 9

Abstract

We propose the metastable emergent dark energy (MEDE) model, a novel phenomenological extension of the phenomenological and generalized emergent dark energy frameworks, in which dark energy exhibits a transitionary behavior, appearing at late times and vanishing toward the future. This model naturally enables a smooth crossing of the phantom dividing line in the dark energy equation of state, as hinted at by recent observations. The MEDE model is defined by a hyperbolic tangent dark energy equation of state $w(z) = -1 - \Delta \tanh[\log_{10}((1+z)/(1+z_t))]$, introducing only two free parameters—the transition redshift z_t and the variation amplitude Δ—allowing both the emergent and transitionary behavior of dark energy. We constrain the MEDE model using a combined dataset of Planck cosmic microwave background (CMB) data, Dark Energy Spectroscopic Instrument (DESI) DR2 baryon acoustic oscillation measurements, and different compilations of Type Ia supernovae, obtaining $z_t = 0.425^{+0.084}_{-0.120}$ and $\Delta = 0.87^{+0.29}_{-0.35}$ (for CMB+DESI+PantheonPlus), indicating a statistically significant deviation from the cosmological constant. Statistical comparisons show that the MEDE model is preferred over ΛCDM by the combined dataset, with $\Delta\mathrm{DIC}_{\mathrm{MEDE-\Lambda CDM}} = -9.29$. The MEDE model performs comparably to the Chevallier–Polarski–Linder (CPL) dynamical dark energy parameterization ($\Delta\mathrm{DIC}_{\mathrm{MEDE-CPL}} = 0.74$), with no strong statistical distinction from CPL using current data. Notably, MEDE preserves the success of ΛCDM in describing early-universe physics and naturally accommodates the phantom-crossing signature indicated by the latest low-redshift observations. The MEDE scenario provides a compelling dark energy phenomenology that may guide us toward interesting theoretical implications.

Unified Astronomy Thesaurus concepts: Cosmology (343); Cosmological models (337); Dark energy (351)

1. Introduction

The standard ΛCDM cosmological model provides an excellent fit to a wide range of astrophysical observations, establishing the cornerstone of modern precision cosmology. Yet it faces several persistent challenges that motivate the exploration of alternative dark-energy paradigms. In particular, the Hubble tension, a 4σ–5σ discrepancy between early- and late-universe measurements of the Hubble constant, and the σ_8 tension concerning the amplitude of matter clustering indicate potential limitations in the standard model's description of dark energy (R.-Y. Guo et al. 2019; L. Verde et al. 2019; S. Vagnozzi 2020, 2023; E. Di Valentino et al. 2021a, 2021b; E. Abdalla et al. 2022; E. Di Valentino 2022; J.-P. Hu & F.-Y. Wang 2023; M. Kamionkowski & A. G. Riess 2023).

Recent results from the Dark Energy Spectroscopic Instrument (DESI) DR2 (M. Abdul Karim et al. 2025) have strengthened the case for dynamical dark energy, reporting a 2.5σ indication that the dark-energy equation of state may cross the phantom divide $w = -1$. This hint, together with earlier indications from other cosmological probes, has motivated a surge of theoretical activity exploring dynamical dark energy scenarios beyond the simple cosmological constant of ΛCDM (W. Giarè et al. 2024a, 2024b; T.-N. Li et al. 2024, 2025; 2025, 2026b; M. Braglia et al. 2025; H. Cheng et al. 2025a, 2026; G.-H. Du et al. 2025, 2026; W. Giarè 2025; G. Gu et al. 2025; J.-Q. Jiang et al. 2025; R. E. Keeley et al. 2025a; C. Li et al. 2025; J.-X. Li & S. Wang 2025; Y.-H. Li & X. Zhang 2025; T. Liu et al. 2025a, 2025b; K. Lodha et al. 2025; E. Özülker et al. 2025; S. Roy Choudhury et al. 2025; R. Shah et al. 2025; E. Silva et al. 2025; E. M. Teixeira et al. 2025; M. van der Westhuizen et al. 2025; W. J. Wolf et al. 2025a, 2026; W. Yang et al. 2025; Y.-M. Zhang et al. 2025; S.-H. Zhou et al. 2025; E. Fazzari et al. 2026; G. G. Luciano et al. 2026; A. Paliathanasis 2026; S. Pan et al. 2026; D. Pedrotti et al. 2026; H. Wang & Y.-S. Piao 2026). However, as cautioned in R. E. Keeley et al. 2025b, the evidence for phantom crossing is not yet definitive. Moreover, even if current data continue to favor such behavior, realizing a crossing of $w = -1$ poses a theoretical challenge, as it cannot be achieved within simple quintessence or phantom models alone.

The emergent dark-energy paradigm offers a compelling alternative by suggesting that dark energy remained subdominant during most of cosmic history, only emerging as a dominant component in the late universe. This idea was first realized phenomenologically in the phenomenological emergent dark energy (PEDE) model, which introduced a smooth

Original content from this work may be used under the terms of the Creative Commons Attribution 4.0 licence. Any further distribution of this work must maintain attribution to the author(s) and the title of the work, journal citation and DOI.

transition in dark-energy density while preserving the parameter count of ΛCDM (X. Li & A. Shafieloo 2019). To allow for more flexibility in the transition shape, the generalized emergent dark energy (GEDE) model was subsequently proposed, incorporating an additional parameter controlling the steepness of emergence (X. Li & A. Shafieloo 2020; J. A. Lozano Torres 2024). Recent studies have revisited PEDE and its generalized version (GEDE) using the latest cosmological data, finding that while PEDE is disfavored by combined datasets (A. Hernández-Almada et al. 2024), GEDE remains consistent with observations and is mildly favored depending on the supernova calibration (V. Sharma et al. 2026); moreover, the preference for dynamical dark energy over a cosmological constant may be sensitive to the choice of priors (G. Payeur et al. 2025). However, both PEDE and GEDE share a fundamental limitation: they do not allow the dark-energy equation of state to cross the phantom divide at $w = -1$, restricting their ability to describe transitions between quintessence ($w > -1$) and phantom ($w < -1$) regimes.

This empirical motivation leads us to propose the metastable emergent dark energy (MEDE) model, which extends the PEDE and GEDE frameworks by allowing smooth phantom crossing while maintaining theoretical consistency. The MEDE parameterization emerges naturally from scalar-field dynamics with noncanonical kinetic terms, particularly in quintom scenarios where phantom and quintessence behaviors coexist. Crucially, MEDE preserves the attractive features of its predecessors: dark energy remains subdominant at early times (safeguarding the well-established high-redshift cosmology), and the model introduces only two additional parameters beyond ΛCDM—the transition redshift z_t and the amplitude of variation Δ—matching the complexity of widely used dynamical dark-energy parameterizations like Chevallier–Polarski–Linder (CPL; M. Chevallier & D. Polarski 2001; E. V. Linder 2003). The CPL parameterization describes the dark-energy equation of state as $w(z) = w_0 + w_a z/(1 + z)$, where w_0 is the present-day value and w_a characterizes its time evolution. While CPL is a widely used empirical tool for describing dark-energy evolution, it remains agnostic about the underlying physics. In contrast, the emergent dark-energy paradigm offers a specific conceptual framework in which dark energy emerges only at late times. MEDE provides a phenomenological realization of this picture that, unlike PEDE (X. Li & A. Shafieloo 2019) and GEDE (X. Li & A. Shafieloo 2020) , allows for phantom crossing.

In this work, we perform a comprehensive test of the MEDE framework by combining the latest Planck cosmic microwave background (CMB) data (Planck Collaboration et al. 2020), DESI baryon acoustic oscillation (BAO) measurements (M. Abdul Karim et al. 2025), and the PantheonPlus Type Ia supernovae (SNe Ia) sample. Our analysis investigates the model's ability to simultaneously address cosmological tensions while accounting for the possible w-crossing behavior suggested by DESI.

The Letter is organized as follows: Section 2 presents the theoretical framework of the MEDE model; Section 3 describes the observational data and statistical methods used in our analysis; Section 4 details the observational constraints and compares them with standard ΛCDM and CPL parameterization; and Section 5 discusses the implications of our findings for fundamental cosmology and future observational programs.

2. Metastable Emergent Dark Energy Model

In a spatially flat Friedmann–Lemaitre–Robertson–Walker (FLRW) universe, the expansion history is governed by the Hubble parameter:

$$H^2(z) = \frac{8\pi G}{3}(\rho_{m0}(1+z)^3 + \rho_{\rm de}(z) + \rho_{r0}(1+z)^4), \quad (1)$$

where ρ_{m0}, ρ_{r0}, and $\rho_{\rm de,0}$ are the present-day energy densities of matter, radiation, and dark energy, respectively. The evolution of dark-energy density for the MEDE model can be written as

$$\rho_{\rm de}(z) = \rho_{\rm de,0}\left[\frac{\cosh\left(\log_{10}\left(\frac{1+z}{1+z_t}\right)\right)}{\cosh\left(\log_{10}\left(\frac{1}{1+z_t}\right)\right)}\right]^{-3\Delta\ln 10}, \quad (2)$$

which directly leads to a dynamical equation of state:

$$w(z) = -1 - \Delta\tanh\left(\log_{10}\left(\frac{1+z}{1+z_t}\right)\right). \quad (3)$$

This formulation ensures that all equations reduce to the ΛCDM limit when $\Delta = 0$, preserving the well-tested success of the standard model at the background level.

To consistently compute cosmological observables like the CMB and matter power spectra, the background dynamics must be complemented by a description of linear perturbations. We consider the linear perturbations of MEDE within the comoving Newtonian gauge. The continuity and Euler equations, governing the evolution of dark-energy inhomogeneities, are derived from the first-order perturbations of the conserved stress–energy–momentum tensor:

$$\delta'_{\rm de} = -(1+w_{\rm de})(\theta_{\rm de} - 3\phi') - 3\mathcal{H}\delta_{\rm de}(c^2_{\rm s,de} - w_{\rm de}) - 9(1+w_{\rm de})(c^2_{\rm s,de} - c^2_{\rm a,de})\mathcal{H}^2\frac{\theta_{\rm de}}{k^2}, \quad (4)$$

$$\theta'_{\rm de} = -(1 - 3c^2_{\rm s,de})\mathcal{H}\theta_{\rm de} + \frac{c^2_{\rm s,de}}{1+w_{\rm de}}k^2\delta_{\rm de} + k^2\psi. \quad (5)$$

Here, primes denote differentiation with respect to conformal time, $\mathcal{H} \equiv a'/a$ is the conformal Hubble parameter, ψ and ϕ are the Bardeen metric potentials, and k is the wavevector magnitude. The density and velocity perturbations for MEDE are $\delta_{\rm de}$ and $\theta_{\rm de}$, respectively, while $c_{\rm s,de}$ and $c_{\rm a,de}$ denote the sound speed and adiabatic sound speed in dark-energy fluid. We fix $c^2_{\rm s,de} = 1$, which is a common choice that prevents unphysical instabilities on small scales and influences the growth of structure, which is crucial for addressing the σ_8 tension. The term $w_{\rm de}$ in these equations is given by Equation (3), intrinsically linking the perturbation evolution to the distinctive background dynamics of the MEDE model.

The MEDE model is thus motivated by a coherent set of theoretical and phenomenological considerations:

1. *Dynamical dark energy and the phantom divide.* The model naturally incorporates a crossing of the phantom divide ($w = -1$), a feature suggested by observations like DESI but challenging for simple quintessence or phantom models. This is inherently encoded in the tanh form of $w(z)$, with the transition centered at z_t.

2. *Emergent and structured evolution.* The "emergent" nature refers to dark energy becoming dominant only at late times. However, unlike a cosmological constant, its density evolves structurally: for $\Delta > 0$, it transitions from phantom-like ($w < -1$) at $z > z_t$ to quintessence-like ($w > -1$) at $z < z_t$, gracefully modifying the expansion history.

In summary, the MEDE model represents a minimal, physically motivated extension to ΛCDM. It combines self-consistently a specific background evolution with its perturbation theory, providing a testable framework for resolving key tensions in modern cosmology. Future data from DESI, Euclid, and CMB-S4 will critically test its viability.

3. Observational Data

The datasets used in the analyses are described below. We present a comprehensive cosmological analysis combining multiple recent observational datasets to constrain the MEDE model. Our dataset compilation includes the following:

BAO. We utilize the latest BAO measurements from the DESI DR2 (DESI Collaboration et al. 2025), which represent the most precise BAO compilation to date. The dataset combines four distinct tracer populations: luminous red galaxies, emission line galaxies, quasars, and the Lyα forest. These measurements provide constraints on three fundamental distance ratios: the transverse comoving distance D_M/r_d, the Hubble distance D_H/r_d, and the volume-averaged distance D_V/r_d, where r_d denotes the sound horizon at the drag epoch. Our analysis properly accounts for the complete covariance structure, including the significant cross-correlation coefficient $r_{M,H}$ between transverse and radial distance measurements, which typically ranges from 0.3 to 0.5 across different redshift bins. This comprehensive BAO dataset is referred to as DESI throughout our work.

SNe Ia. We employ two independent SN Ia compilations to constrain the late-time expansion history. (i) We use the full PantheonPlus sample (D. Scolnic et al. 2022), consisting of 1701 high-quality light curves from 1550 spectroscopically confirmed SNe Ia spanning $0.01 < z < 2.26$. To mitigate potential systematics from low-redshift calibration uncertainties, we exclude the calibration subsample at $z < 0.01$ and rigorously incorporate the full covariance matrix,[7] which captures both statistical errors and systematic correlations. The final sample of 1485 SN Ia provides a robust Hubble diagram for cosmological inference. (ii) We employ the fully recalibrated DES-Dovekie supernova sample (B. Popovic et al. 2025), derived from a comprehensive reanalysis of the Dark Energy Survey (DES) 5 yr SN Ia. This sample incorporates several key improvements from DES Collaboration et al. (2024), including an enhanced photometric cross calibration, the use of recent white dwarf observations for calibration across surveys, a retrained SALT3 light-curve model, and a corrected host galaxy color law. The final DES-Dovekie dataset consists of approximately 1600 likely SNe Ia from DES and about 200 low-redshift supernovae from external surveys, providing a robust foundation for constraining cosmological models. These datasets are labeled *PantheonPlus* and *DES-Dovekie*, respectively.

CMB. Our CMB constraints are derived from the Planck 2018 legacy data (Planck Collaboration et al. 2020), including high-ℓ temperature and polarization spectra (TT+TE+EE) and low-ℓ temperature (TT) and polarization (EE) likelihoods. These measurements precisely determine the acoustic peak structure and are sensitive to fundamental cosmological parameters including the baryon density, matter content, and expansion history. Additionally, we include CMB lensing constraints from the combined Planck PR4 (NPIPE) reconstruction (J. Carron et al. 2022) and Atacama Cosmology Telescope DR6 results (N. MacCrann et al. 2024; M. S. Madhavacheril et al. 2024; F. J. Qu et al. 2024). The lensing potential power spectrum $C_\ell^{\phi\phi}$ probes the integrated matter distribution and provides complementary constraints on late-time structure growth. The combined dataset, denoted as *CMB*, comprises Planck 2018 TT, TE, EE spectra together with the Planck+ACT lensing likelihood.

The theoretical framework of the MEDE model, as defined by its background evolution (Equations (2) and (3)) and perturbation equations, is implemented numerically to enable confrontation with observational data. We incorporate this model into a modified version of the CAMB Boltzmann solver (A. Lewis et al. 2000). Bayesian parameter estimation is subsequently performed using the Cobaya[8] framework (J. Torrado & A. Lewis 2021). The Markov Chain Monte Carlo (MCMC) sampling convergence is rigorously assessed via the Gelman–Rubin criterion (A. Gelman & D. B. Rubin 1992), requiring $R - 1 < 0.01$ for all parameters. We adopt uniform priors on the cosmological parameter set $\{\Omega_b h^2, \Omega_c h^2, \tau_{\rm reio}, n_s, \log(10^{10}A_s), \Delta, z_t\}$, with the resulting posterior distributions analyzed using the GetDist package.[9] This comprehensive approach enables the robust determination of one-dimensional (1D) marginalized constraints and two-dimensional (2D) joint confidence regions for all model parameters.

We employ the deviance information criterion (DIC; D. J. Spiegelhalter et al. 2002; A. R. Liddle 2007) for model comparison. DIC is defined as

$$\mathrm{DIC} = \bar{D} + p_D, \tag{6}$$

where $\bar{D}$ is the posterior mean of the deviance $D(\theta) = -2\ln\mathcal{L}(\theta)$, and $p_D = \bar{D} - D(\bar{\theta})$ is the effective number of parameters. By using the effective number of parameters, DIC overcomes the problem of other information criteria like Akaike criterion, in that it does not discount parameters that are unconstrained by the data. Under the Gaussian likelihood assumption, $D(\theta)$ is equivalent to $\chi^2(\theta)$. Thus, DIC can be expressed in terms of χ^2 as

$$\mathrm{DIC} = 2\langle\chi^2(\theta)\rangle - \chi^2(\bar{\theta}), \tag{7}$$

where $\langle\chi^2(\theta)\rangle$ is the mean of χ^2 over the posterior samples, and $\chi^2(\bar{\theta})$ is χ^2 evaluated at the posterior mean of the parameters. A smaller DIC indicates a better balance between goodness of fit and model complexity.

Our analysis of the MEDE model, combining the latest CMB, DESI BAO, and SN Ia (PantheonPlus and DES-Dovekie) datasets, yields robust constraints on key cosmological parameters. The 1D marginalized posterior distributions and 2D joint confidence regions are displayed in Figure 1, while numerical results are summarized in Table 1. For comparative assessment, Figure 2 displays the posterior

[7] https://github.com/PantheonPlusSH0ES/DataRelease

[8] https://github.com/CobayaSampler/cobaya

[9] https://github.com/cmbant/getdist

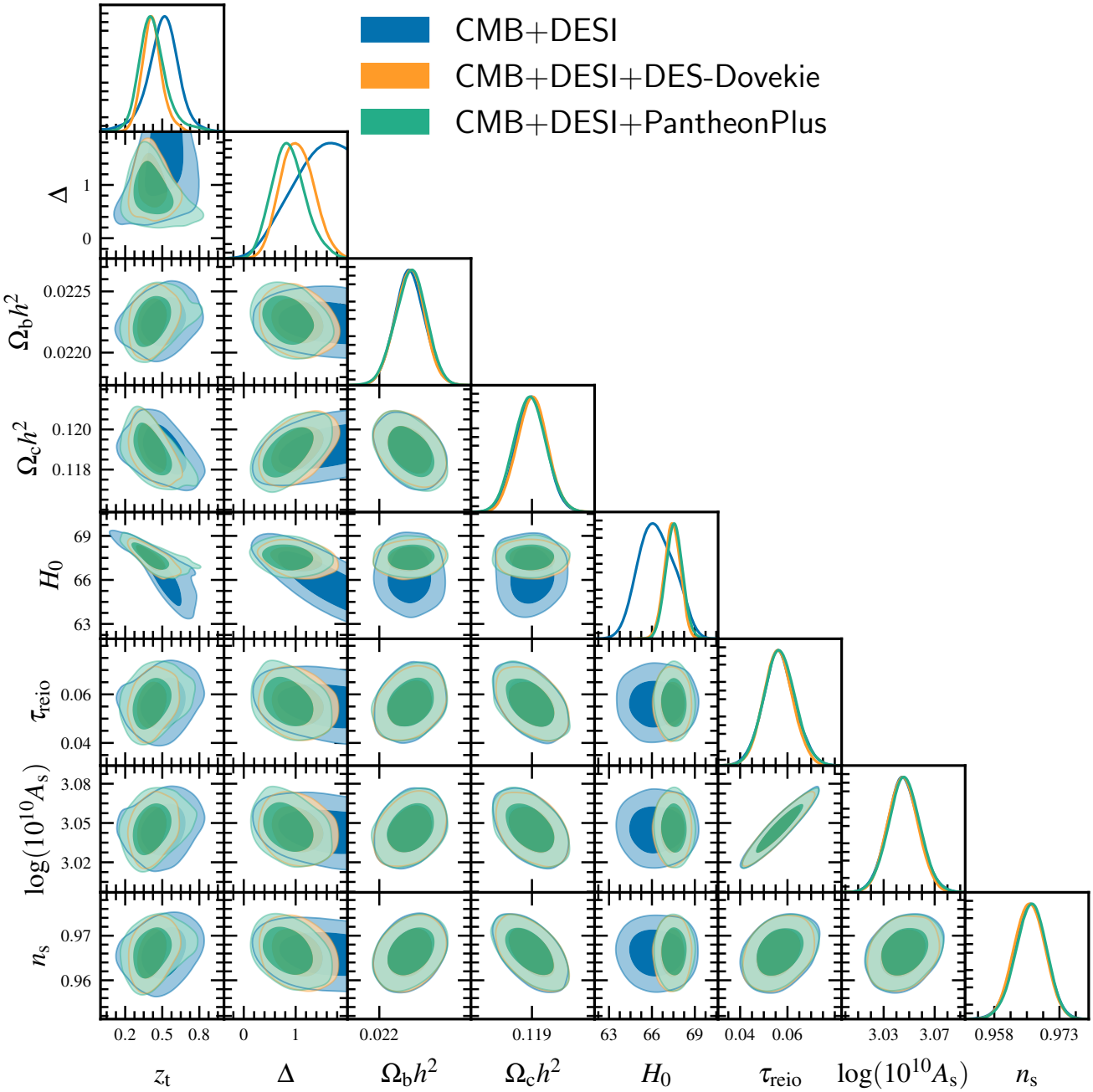

Figure 1. Constraints on the cosmological parameters of the MEDE model. The panels show the one-dimensional posterior distributions and two-dimensional joint confidence regions (68% and 95%) for the core cosmological and MEDE model parameters, derived from the combination of CMB, DESI BAO, DES-Dovekie, and PantheonPlus supernova data.

distributions of the total χ^2 for the three cosmological models under consideration, obtained from the joint CMB+DESI DR2 +PantheonPlus analysis.

The most striking evidence for the emergent nature of dark energy comes from the highly consistent constraint on the transition redshift z_t obtained from two complementary dataset combinations: $z_t = 0.418^{+0.070}_{-0.085}$ (CMB+DESI+DES-Dovekie) and $z_t = 0.425^{+0.084}_{-0.120}$ (CMB+DESI+PantheonPlus). This remarkable agreement strongly indicates that the dark-energy transition occurs squarely within the epoch of cosmic acceleration onset ($z \sim 0.5$), suggesting a fundamental connection between the emergence of dark-energy dominance and the recent acceleration phase. Furthermore, the positive values of $\Delta = 1.03 \pm 0.32$ and $0.87^{+0.29}_{-0.35}$ from the respective datasets consistently indicate a specific evolutionary pattern: dark energy evolves from phantom-like behavior ($w < -1$) at $z > z_t$ to quintessence-like behavior ($w > -1$) at $z < z_t$. This crossing of the phantom divide, while challenging for simple scalar-field models, arises naturally in the MEDE framework through its hyperbolic parameterization, which can be mapped onto quintom scenarios with noncanonical kinetic terms. The concordance between these independent datasets significantly reinforces the robustness of this dynamical dark-energy signature.

The addition of DESI BAO data serves as a powerful low-redshift anchor, breaking geometric degeneracies through its precise measurements of $D_M(z)/r_d$ and $H(z)r_d$ across multiple redshifts. Within the CMB+DESI dataset, this leads to tightly

Table 1
Constraints on Cosmological Parameters for the Flat MEDE Model

Model	MEDE Model		
Data	CMB+DESI	CMB+DESI+DES-Dovekie	CMB+DESI+PantheonPlus
z_t	$0.500^{+0.130}_{-0.110}$	$0.418^{+0.070}_{-0.085}$	$0.425^{+0.084}_{-0.120}$
Δ	>1.12	1.03 ± 0.32	$0.87^{+0.29}_{-0.35}$
$\Omega_b h^2$	0.02226 ± 0.00012	0.02226 ± 0.00012	0.02226 ± 0.00013
$\Omega_c h^2$	0.11895 ± 0.00078	0.11902 ± 0.00077	0.11890 ± 0.00081
$\log(10^{10}A_s)$	3.046 ± 0.012	3.045 ± 0.012	3.046 ± 0.012
n_s	0.9662 ± 0.0036	0.9661 ± 0.0035	0.9664 ± 0.0035
τ_{reio}	0.0564 ± 0.0067	0.0561 ± 0.0062	0.0567 ± 0.0066
H_0 (km s^{-1} Mpc^{-1})	$66.30^{+1.20}_{-1.40}$	67.43 ± 0.56	67.56 ± 0.58
Ω_m	0.3230 ± 0.0120	0.3122 ± 0.0055	0.3108 ± 0.0056
σ_8	0.8020 ± 0.0120	0.8116 ± 0.0073	0.8120 ± 0.0079
r_{drag}	147.51 ± 0.21	147.49 ± 0.20	147.51 ± 0.20
χ^2_{min}	11006.35	12632.67	12406.45
$\Delta\chi^2_{MEDE\text{-}\Lambda CDM}$	−1.65	−8.43	−3.94
$\Delta\chi^2_{MEDE\text{-}CPL}$	4.22	4.53	3.39
$\Delta DIC_{MEDE\text{-}\Lambda CDM}$	−6.53	−11.36	−9.29
$\Delta DIC_{MEDE\text{-}CPL}$	1.71	1.32	0.74

Note. Results are shown for the CMB+DESI, CMB+DESI+DES-Dovekie, and CMB+DESI+PantheonPlus datasets, and we also include the minimum χ^2, $\Delta\chi^2$, and ΔDIC values relative to the ΛCDM and CPL models.

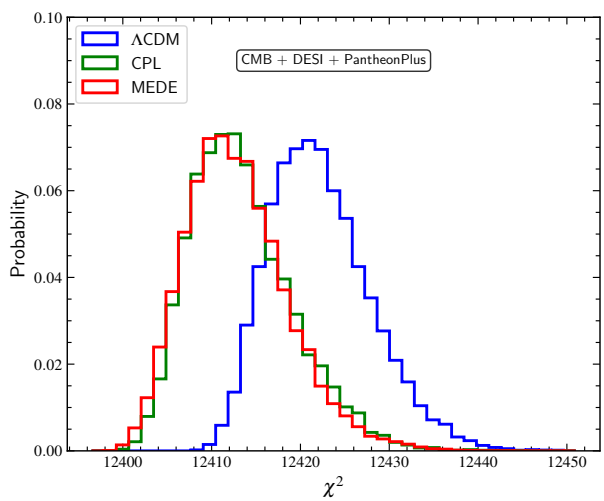

Figure 2. χ^2 distributions from MCMC chains for ΛCDM (blue), CPL dynamical dark energy (green), and MEDE (red) models, constrained by CMB +DESI DR2+PantheonPlus data.

constrained parameters, with $H_0 = 66.30^{+1.20}_{-1.40}$ km s^{-1} Mpc^{-1} and a transition parameter $\Delta > 1.12$. The BAO distance measurements strongly constrain the sound horizon scale $r_{drag} = 147.51 \pm 0.21$ Mpc, which remains highly consistent across different data combinations—further attesting to the stability of early-universe physics in the MEDE framework. The MEDE model also shows improved fit quality over ΛCDM in this dataset, as reflected by $\Delta\chi^2_{MEDE-\Lambda CDM} = -1.65$, $\Delta DIC_{MEDE-\Lambda CDM} = -6.53$.

The subsequent inclusion of DES-Dovekie and PantheonPlus supernova data further refines the measurement of the cosmic expansion history. Supernovae provide direct observations of the luminosity distance, which integrates over the Hubble function $H(z)$. Remarkably, the parameter constraints from the CMB+DESI +DES-Dovekie and CMB+DESI+PantheonPlus combinations show a high degree of consistency: the transition parameter $\Delta = 1.03 \pm 0.32$ and $0.87^{+0.29}_{-0.35}$, the Hubble constant $H_0 = 67.43 \pm 0.56$ km s^{-1} Mpc^{-1} and 67.56 ± 0.58 km s^{-1} Mpc^{-1}, and the matter density parameter $\Omega_m = 0.3122 \pm 0.0055$ and 0.3108 ± 0.0056, respectively. This consistency underscores the robustness of the MEDE framework against different cosmological probes, especially given the distinct systematics and redshift coverages of the DES-Dovekie and PantheonPlus samples. Furthermore, the addition of supernova data leads to a significant improvement in the goodness of fit for the MEDE model over ΛCDM: for the CMB+DESI+DES-Dovekie combination, $\Delta\chi^2_{MEDE-\Lambda CDM} = -8.43$ and $\Delta DIC_{MEDE-\Lambda CDM} = -11.36$; for the CMB+DESI+PantheonPlus combination, $\Delta\chi^2_{MEDE-\Lambda CDM} = -3.94$ and $\Delta DIC_{MEDE-\Lambda CDM} = -9.29$. These results collectively indicate a preference for the MEDE model over ΛCDM when late-time observational data are incorporated.

Compared with the widely adopted CPL parameterization, the statistical evidence remains inconclusive. The positive $\Delta\chi^2_{MEDE\text{-}CPL}$ values indicate that, in terms of the minimum χ^2, the CPL parameterization provides a slightly better fit to the data than the MEDE model. This is further supported by the DIC: since a lower DIC value is preferred, the positive $\Delta DIC_{MEDE\text{-}CPL}$ values imply that, after accounting for model complexity, the data show a mild preference for CPL over MEDE. It is important to note, however, that all ΔDIC values fall below the conventional threshold of 5 for substantial evidence. Therefore, current data do not provide strong statistical grounds to decisively distinguish between the MEDE and CPL models.

The stability of primordial parameters across different dataset combinations demonstrates that the MEDE model retains the success of ΛCDM in describing early-universe physics, while introducing additional dynamical freedom only at late times. This clear separation of scales is a desirable

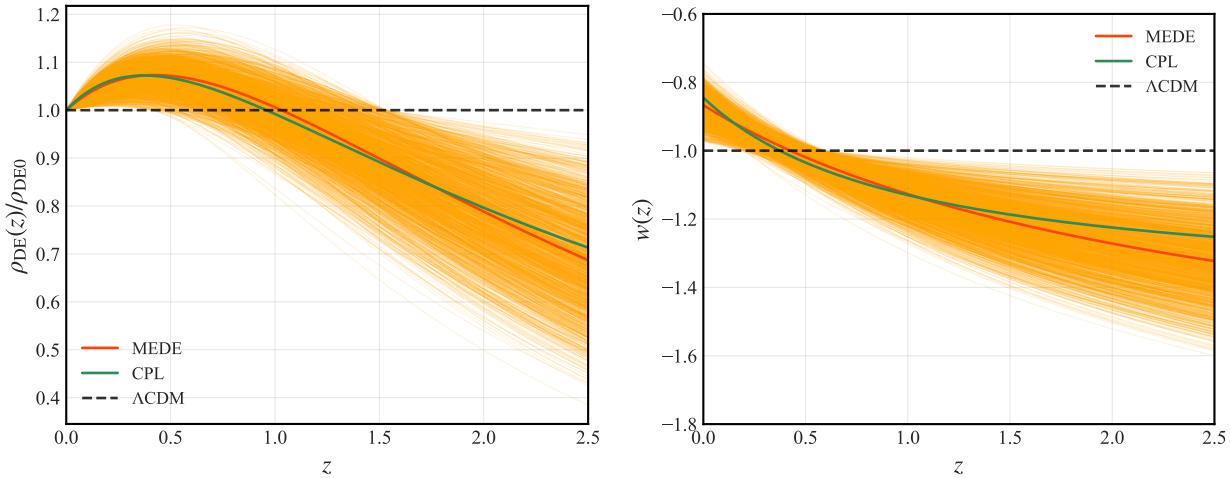

Figure 3. Redshift evolution of the dark-energy sector. Left: the dark-energy density $\rho_{DE}(z)/\rho_{DE0}$. Right: the equation of state $w_{DE}(z)$. The red solid line represents the best-fit MEDE model (CMB+DESI+PantheonPlus). The light-orange region shows the 2σ confidence region derived from MCMC chains, illustrating the posterior distribution of parameters. The green solid line shows the CPL parameterization ((CMB+DESI+PantheonPlus best-fit), and the black dashed line represents ΛCDM. The MEDE model exhibits a smooth transition around $z_t \sim 0.42$, crossing the phantom divide $w = -1$ from phantom-like ($w < -1$) at high redshifts to quintessence-like ($w > -1$) at low redshifts.

feature for any dark-energy extension, as it avoids interference with the well-constrained physics of the primordial universe.

Overall, the MEDE framework presents a compelling, theoretically motivated alternative to ΛCDM, as evidenced by the negative $\Delta\chi^2$ and ΔDIC values relative to the standard model. Its performance is comparable to the widely used CPL parameterization, with the small ΔDIC values indicating no strong statistical preference for either model. This positions MEDE as a viable dynamical dark-energy scenario worthy of further investigation with future, more precise observational data.

4. Results and Discussion

Figure 3 illustrates the redshift evolution of the dark-energy sector in the MEDE framework. The left panel shows the dark-energy density $\rho_{DE}(z)/\rho_0$, while the right panel displays the corresponding equation of state $w_{DE}(z)$. The thick purple solid line represents the best-fit MEDE model from the CMB+DESI +PantheonPlus dataset, with $z_t = 0.425$ and $\Delta = 0.87$, while the surrounding light-purple region indicates the 2σ confidence levels derived from MCMC chains. For comparison, the CPL parameterization with $w_0 = -0.845$ and $w_a = -0.57$ best fit from CMB+DESI+PantheonPlus dataset is shown as a red solid line, and the ΛCDM limit is shown as a black dashed line. The constrained transition around $z_t \sim 0.42$ reveals a smooth crossing of the phantom divide ($w = -1$), where dark energy evolves from phantom-like behavior ($w < -1$) at high redshifts to quintessence-like behavior ($w > -1$) at low redshifts. This figure visually demonstrates the unique evolutionary pattern of the MEDE model, which naturally accommodates phantom crossing while maintaining theoretical consistency across the entire redshift range. CPL parameterization by its construction—as a first-order Taylor expansion in $a(t)$—has limited range of applicability. The idea here is that once we formulate a theoretical model of dark energy, its effective evolving equation of state $w(z) \equiv w(a(t))$ when Taylor expanded around $a = 1$ should have w_0 and w_a coefficients coinciding with the best fitted CPL model. Interestingly, when we do such an exercise with MEDE, i.e., expanding Equation (3), we obtain the following correspondence between CPL and MEDE:

$$w_0 = -1 + \Delta \tanh[\log_{10}(1 + z_t)], \tag{8}$$

$$w_a = -\frac{1}{\ln 10}\Delta \operatorname{sech}^2[\log_{10}(1 + z_t)]. \tag{9}$$

Substituting the central values of Δ and z_t fitted to the (CMB +DESI+DES-Dovekie) data (see Table 1), one obtains $w_0 = -0.845^{+0.076}_{-0.067}$, $w_a = -0.44^{+0.13}_{-0.13}$, which is within 1σ of the DESI (M. Abdul Karim et al. 2025) best fit $w_0 = -0.838 \pm 0.055$, $w_a = -0.62^{+0.22}_{-0.19}$. This explains the similarity in performance between CPL and MEDE in the redshift range probed by current data: they can be viewed as two sides of the same coin, both conveying the message that an evolving equation of state should be taken seriously as an alternative to the ΛCDM model.

Figure 4 shows the redshift evolution of the dark-energy sector for MEDE, CPL, and ΛCDM, with the left panel displaying the dark-energy density $\rho_{DE}(z)/\rho_{DE,0}$ and the right panel the equation of state $w_{DE}(z)$. As illustrated, the MEDE equation of state (best fit to the current data) remains well behaved asymptotically into the infinite future, whereas CPL can evolve to values beyond $w = 1$, which are difficult to interpret physically. This highlights an important difference: MEDE is constructed from a physically motivated density evolution, in which dark energy appears and then disappears, rather than from an assumed form of the equation of state.

Beyond statistical comparison, it is also instructive to consider how these parameterizations relate to underlying physical models. Studies such as those by W. J. Wolf & P. G. Ferreira (2023), Z. Bayat & M. P. Hertzberg (2025), W. J. Wolf et al. (2024), and D. Shlivko et al. (2025) show that CPL may struggle to reconstruct the true equation of state of certain scalar-field models, while W. J. Wolf et al. (2025b) demonstrate it can still reproduce key observables within current uncertainties. More generally, the limitations of fixed parametric forms have long motivated non-parametric approaches: for example, CPL fails to fit certain braneworld models (A. Shafieloo et al. 2006) and cannot adequately capture sharp transitions in the equation of state (T. Holsclaw et al. 2010). CPL remains a flexible empirical

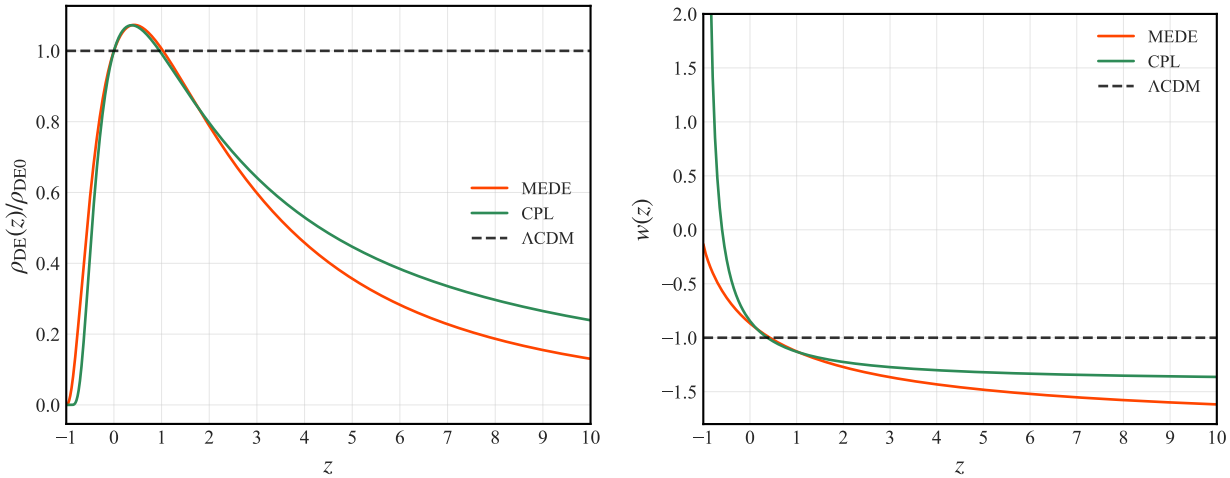

Figure 4. Redshift evolution of the dark-energy sector for MEDE, CPL, and ΛCDM. Left: dark-energy density $\rho_{DE}(z)/\rho_{DE,0}$. Right: equation of state $w_{DE}(z)$. The red solid line shows the best-fit MEDE model (CMB+DESI+PantheonPlus). The green solid line is the best-fit CPL parameterization, and the black dashed line is ΛCDM. The evolution is shown from the distant past $z \approx 10$ to the asymptotic future $z \to -1$, illustrating the distinct behaviors of each model at late times.

tool, whereas MEDE is explicitly rooted in the emergent dark-energy paradigm—preserving the emergence feature of PEDE/GEDE while allowing phantom crossing. Thus, MEDE should be seen not as a replacement for CPL, but as a complementary framework grounded in a specific physical picture.

While both CPL and MEDE are currently phenomenological, CPL by construction has a more limited redshift range of validity than MEDE. Work is under way to ground MEDE in a concrete microphysical scenario involving scalar fields, which would further elevate it from a phenomenological proposal to a more fundamentally motivated one.

5. Conclusion

We have proposed the MEDE model, a novel phenomenological extension of the PEDE and GEDE frameworks, in which dark energy exhibits both emergent and transitionary behavior, appearing dynamically at late times and potentially vanishing toward the future. This construction provides a simple yet flexible framework in which dark energy is not a rigid cosmological constant, but rather a metastable component whose effective contribution to the cosmic expansion can evolve nontrivially across cosmic time. In particular, the model naturally accommodates scenarios in which dark energy effectively fades away in the far future, thereby opening qualitatively new perspectives on the ultimate fate of the Universe.

The MEDE model is defined by the hyperbolic equation of state $w(z) = -1 - \Delta \tanh[\log_{10}((1+z)/(1+z_t))]$, which introduces only two additional free parameters beyond ΛCDM, namely the transition redshift z_t and the variation amplitude Δ. Despite its minimal parameterization, the model successfully captures both the emergent onset of dark-energy domination and a transitionary behavior that allows for a smooth and physically motivated crossing of the phantom divide line. Such phantom-crossing behavior has been hinted at by several recent low-redshift observations from BAO and supernovae, and MEDE provides a coherent phenomenological realization of this possibility without introducing pathologies at the background level.

Constraining the model using a combined dataset of Planck CMB, DESI DR2 BAO, and different compilations of SNe Ia, we obtain $z_t = 0.425^{+0.084}_{-0.120}$ and $\Delta = 0.87^{+0.29}_{-0.35}$ (for CMB+DESI+PantheonPlus), indicating a statistically significant deviation from the cosmological constant scenario. Statistical comparisons show that the MEDE model is preferred over ΛCDM by the combined dataset, with $\Delta\mathrm{DIC}_{\mathrm{MEDE-\Lambda CDM}} = -9.29$, while it performs comparably to the CPL dynamical dark-energy parameterization ($\Delta\mathrm{DIC}_{\mathrm{MEDE-CPL}} = 0.74$), with no strong statistical distinction from CPL using current data. In this sense, MEDE emerges as a competitive and equally viable alternative to CPL and other compelling dynamical dark-energy models.

Importantly, the MEDE framework preserves the well-established successes of ΛCDM in describing early-universe physics, while extending the late-time sector in a controlled and testable manner. The combination of emergent behavior, transitionary dynamics, and phantom-crossing capability makes MEDE a particularly appealing phenomenological scenario. Beyond its empirical performance, the model may serve as guidance toward more fundamental theoretical constructions, potentially pointing to underlying metastable vacuum structures, interacting sectors, multifield models, or modified gravitational dynamics responsible for the effective behavior captured by the parameterization. Owing to space limitations, the physical origin framework, action, and consistency check are not covered in this Letter. A comprehensive presentation of these aspects of the MEDE model will be provided in future work.

Looking ahead, forthcoming high-precision cosmological observations will be crucial in clarifying the current hints of dynamical dark energy. Future surveys with improved sensitivity to low-redshift expansion history and structure growth will be able to discriminate more decisively between ΛCDM, CPL, MEDE, and other competing models. In this context, the MEDE scenario provides a minimal, flexible, and observationally testable framework that stands as a competitive alternative in the exploration of the nature and fate of dark energy.

Acknowledgments

This work was supported by the National Key R&D Program of China (No. 2024YFC2207400) and the Science Research Project of Hebei Education Department No.

BJK2024134. This work benefits from the high performance computing clusters at College of Physics, Hebei Normal University, and the Chutian Scholars Program in Hubei Province (X2023007). A.S. would like to acknowledge the support by National Research Foundation of Korea NRF2021M3F7A1082056 and the support of the Korea Institute for Advanced Study. M.B. was supported by the Polish National Science Centre grant 2023/50/A/ST9/00579 and by COST Action CA21136—"Addressing observational tensions in cosmology with systematics and fundamental physics (CosmoVerse)."

ORCID iDs

Xiaolei Li https://orcid.org/0000-0002-2154-0394
Tian-Nuo Li https://orcid.org/0009-0004-6982-4021
Guo-Hong Du https://orcid.org/0009-0005-6921-3201
Arman Shafieloo https://orcid.org/0000-0001-6815-0337
Marek Biesiada https://orcid.org/0000-0003-1308-7304

References

Abdalla, E., Abellán, G. F., Aboubrahim, A., et al. 2022, JHEAp, 34, 49
Abdul Karim, M., Aguilar, J., Ahlen, S., et al. 2025, PhRvD, 112, 083515
Bayat, Z., & Hertzberg, M. P. 2025, JCAP, 08, 065
Braglia, M., Chen, X., & Loeb, A. 2025, JCAP, 2025, 064
Carron, J., Mirmelstein, M., & Lewis, A. 2022, JCAP, 2022, 039
Cheng, H., Di Valentino, E., Escamilla, L. A., Sen, A. A., & Visinelli, L. 2025a, JCAP, 09, 031
Cheng, H., Pan, S., & Di Valentino, E. 2026, ApJ, 999, 190
Chevallier, M., & Polarski, D. 2001, IJMPD, 10, 213
DES Collaboration, Abbott, T. M. C., Acevedo, M., et al. 2024, ApJL, 973, L14
DESI Collaboration, Abdul-Karim, M., Aguilar, J., et al. 2025, PhRvD, 112, 083515
Di Valentino, E. 2022, Univ, 8, 399
Di Valentino, E., Anchordoqui, L. A., Akarsu, Ö., et al. 2021a, APh, 131, 102605
Di Valentino, E., Mena, O., Pan, S., et al. 2021b, CQGra, 38, 153001
Du, G.-H., Li, T.-N., Liu, T., Zhang, J.-F., & Zhang, X. 2026, arXiv:2602.03110
Du, G.-H., Li, T.-N., Wu, P.-J., Zhang, J.-F., & Zhang, X. 2025, arXiv:2507.16589
Fazzari, E., Giarè, W., & Di Valentino, E. 2026, ApJL, 996, L5
Gelman, A., & Rubin, D. B. 1992, StaSc, 7, 457
Giarè, W. 2025, PhRvD, 112, 023508
Giarè, W., Najafi, M., Pan, S., Di Valentino, E., & Firouzjaee, J. T. 2024a, JCAP, 10, 035
Giarè, W., Sabogal, M. A., Nunes, R. C., & Di Valentino, E. 2024b, PhRvL, 133, 251003
Gu, G., Wang, X., Wang, Y., et al. 2025, NatAs, 9, 1879
Guo, R.-Y., Zhang, J.-F., & Zhang, X. 2019, JCAP, 02, 054
Hernández-Almada, A., Mendoza-Martínez, M. L., García-Aspeitia, M. A., & Motta, V. 2024, PDU, 46, 101668
Holsclaw, T., Alam, U., Sansó, B., et al. 2010, PhRvD, 82, 103502
Hu, J.-P., & Wang, F.-Y. 2023, Univ, 9, 94
Jiang, J.-Q., Giarè, W., Gariazzo, S., et al. 2025, JCAP, 01, 153
Kamionkowski, M., & Riess, A. G. 2023, ARNPS, 73, 153
Keeley, R. E., Abazajian, K. N., Kaplinghat, M., & Shafieloo, A. 2025a, PhRvD, 112, 043501
Keeley, R. E., Shafieloo, A., & Matthewson, W. L. 2025b, arXiv:2506.15091
Lewis, A., Challinor, A., & Lasenby, A. 2000, ApJ, 538, 473
Li, C., Wang, J., Zhang, D., Saridakis, E. N., & Cai, Y.-F. 2025, JCAP, 08, 041
Li, J.-X., & Wang, S. 2025, EPJC, 85, 1308
Li, T.-N., Du, G.-H., Li, Y.-H., et al. 2025, SCPMA, 69, 210413
Li, T.-N., Giarè, W., Du, G.-H., et al. 2026b, arXiv:2601.07361
Li, T.-N., Li, Y.-H., Du, G.-H., et al. 2025, EPJC, 85, 608
Li, T.-N., Wu, P.-J., Du, G.-H., et al. 2024, ApJ, 976, 1
Li, X., & Shafieloo, A. 2019, ApJL, 883, L3
Li, X., & Shafieloo, A. 2020, ApJ, 902, 58
Li, Y.-H., & Zhang, X. 2025, JCAP, 12, 018
Liddle, A. R. 2007, MNRAS, 377, L74
Linder, E. V. 2003, PhRvL, 90, 091301
Liu, T., Li, X., & Wang, J. 2025a, ApJ, 988, 243
Liu, T., Li, X., Xu, T., Biesiada, M., & Wang, J. 2025b, EPJC, 85, 1351
Lodha, K., Calderon, R., R., Matthewson, W. L., et al. 2025, PhRvD, 112, 083511
Lozano Torres, J. A. 2024, MNRAS, 533, 1865
Luciano, G. G., Paliathanasis, A., & Saridakis, E. N. 2026, JHEAp, 49, 100427
MacCrann, N., Sherwin, B. D., Qu, F. J., et al. 2024, ApJ, 966, 138
Madhavacheril, M. S., Qu, F. J., Sherwin, B. D., et al. 2024, ApJ, 962, 113
Özülker, E., Di Valentino, E., & Giarè, W. 2025, arXiv:2506.19053
Paliathanasis, A. 2026, arXiv:2601.02789
Pan, S., Paul, S., Saridakis, E. N., & Yang, W. 2026, PhRvD, 113, 023515
Payeur, G., McDonough, E., & Brandenberger, R. 2025, PhRvD, 111, 123541
Pedrotti, D., Escamilla, L. A., Marra, V., Perivolaropoulos, L., & Vagnozzi, S. 2026, PhRvD, 113, 043507
Planck Collaboration, Aghanim, N., Akrami, Y., et al. 2020, A&A, 641, A6
Popovic, B., Shah, P., Kenworthy, W.D., et al. 2025, arXiv:2511.07517
Qu, F. J., Sherwin, B. D., Madhavacheril, M. S., et al. 2024, ApJ, 962, 112
Roy Choudhury, S., Okumura, T., & Umetsu, K. 2025, ApJL, 994, L26
Scolnic, D., Brout, D., Carr, A., et al. 2022, ApJ, 938, 113
Shafieloo, A., Alam, U., Sahni, V., & Starobinsky, A. A. 2006, MNRAS, 366, 1081
Shah, R., Mukherjee, P., & Pal, S. 2025, MNRAS, 542, 2936
Sharma, V., Chaudhary, H., & Kolekar, S. 2026, JHEAp, 51, 100518
Shlivko, D., Steinhardt, P. J., & Steinhardt, C. L. 2025, JCAP, 2025, 054
Silva, E., Sabogal, M. A., Scherer, M., et al. 2025, PhRvD, 111, 123511
Spiegelhalter, D. J., Best, N. G., Carlin, B. P., & Van Der Linde, A. 2002, J. R. Stat. Soc. Ser. B Methodol, 64, 583
Teixeira, E. M., Giarè, W., Hogg, N. B., et al. 2025, PhRvD, 112, 023515
Torrado, J., & Lewis, A. 2021, JCAP, 2021, 057
Vagnozzi, S. 2020, PhRvD, 102, 023518
Vagnozzi, S. 2023, Univ, 9, 393
van der Westhuizen, M., Abebe, A., & Di Valentino, E. 2025, PDU, 50, 102121
Verde, L., Treu, T., & Riess, A. G. 2019, NatAs, 3, 891
Wang, H., & Piao, Y.-S. 2026, arXiv:2601.06656
Wolf, W. J., & Ferreira, P. G. 2023, PhRvD, 108, 103519
Wolf, W. J., Ferreira, P. G., & García-García, C. 2026, PhRvD, 113, 023551
Wolf, W. J., García-García, C., Anton, T., & Ferreira, P. G. 2025a, PhRvL, 135, 081001
Wolf, W. J., García-García, C., Bartlett, D. J., & Ferreira, P. G. 2024, PhRvD, 110, 083528
Wolf, W. J., García-García, C., & Ferreira, P. G. 2025b, JCAP, 05, 034
Yang, W., Zhang, S., Mena, O., Pan, S., & Di Valentino, E. 2025, arXiv:2508.19109
Zhang, Y.-M., Li, T.-N., Du, G.-H., et al. 2025, arXiv:2510.12627
Zhou, S.-H., Li, T.-N., Du, G.-H., et al. 2025, PhRvD, 112, 123532